HETEROCYCLES, Vol. 104, No. 4, 2022, pp. 667 - 688. © 2022 The Japan Institute of Heterocyclic Chemistry
Received, 9th November, 2021, Accepted, 11th January, 2022, Published online, 21st January, 2022
DOI: 10.3987/COM-21-14586

DESIGN, SYNTHESIS AND BIOLOGICAL EVALUATION OF NOVEL INDOLE-CONTAINING SORAFENIB DERIVATIVES

Sili Fan,[1#] Yihong Fu,[1#] Siyu Tang,[1] Danping Chen,[1] Zhurui Li,[1] Chengpeng Li,[1] Lihui Shao,[1] Zhenchao Wang,[1,2,3]* and Guiping Ouyang[1,2,3]*

[1] School of Pharmaceutical Sciences, Guizhou University, Guizhou Guiyang, 550025, China; [2] Key Laboratory of Green Pesticide and Agricultural Bioengineering, Ministry of Education, Guiyang, 550025, China; [3] Guizhou Engineering Laboratory for Synthetic Drugs, Guiyang, 550025, China. [#] These authors contributed equally to this work. Email: wzc.4884@163.com, gpouyang@gzu.edu.cn

Abstract – Based on the molecular structure of sorafenib, a series of novel indole (ketone) semicarbazide analogs (**1-30**) have been designed and synthesized. All new compounds were identified by ^{1}H, ^{13}C NMR and HRMS, and their antiproliferative activity on four cancer cell lines A549, PC-3, K562 and HepG2 were evaluated. In particular, compared with the positive control sorafenib (18.92 μmol/L), compounds **4**, **6** and **20** showed two- to three-fold improvement in inhibiting the proliferation of PC-3 cells with IC_{50} values of 6.75, 8.03 and 8.77 μmol/L respectively. *In vitro* activity evaluation experiments showed that compound **6** could significantly inhibit the proliferation and colony formation of PC-3 cells, induce apoptosis and arrest the cells in the G2/M phase. Finally, western blot speculated that compound **6** may affect the signal transduction of downstream signaling pathway PI3K/Akt by affecting EGFR protein and autophosphorylation thereby promoting cell apoptosis and inhibiting cell growth. These results provide important information for the development of new anti-cancer drugs.

INTRODUCTION

Cancer is a major public health problem worldwide and is the second leading cause of death in the world.[1] In recent years, the design and development of multi-target drugs has become the current research trend.[2,3]

Sorafenib is known as the excellent inhibitory activity to a variety of kinases,[4,5] including vascular endothelial growth factor receptor (VEGFR), platelet-derived growth factor receptor-β (PDGFR-β), stem cell growth factor receptor (c-kit), Fms-like tyrosine kinase-3 (FLT-3).[6] Therefore, the research on the mechanism of action of sorafenib and its derivatives has also received extensive attention.[7–12]

EGFR (epidermal growth factor receptor) is a reasonable target for cancer treatment because it is usually found at high levels in various solid tumors. It is expressed, and is related to the control of cell survival, proliferation, metastasis and angiogenesis.[13,14] The study of EGFR as a therapeutic target is an important part of the field of cancer treatment,[15] and it has high activity against a variety of tumor,[16,17] such as lung cancer,[18] gastric cancer,[19] breast cancer,[20] etc. From a synthetic point of view, the compounds whose modification of this structure focused on the urea structural own better activity.[21] In order to explore the EGFR inhibition ability, this research continues to further reform the structure of sorafenib based on literature research.

The hydrazone structure was introduced as a pharmacophore into some antitumor drugs,[22] and produces antitumor activity that promotes the apoptosis of cancer cells and antiproliferation.[23,24] Studies have shown that indole has been used as a privileged scaffold in the anticancer agents design,[25] and indole derivatives have the potential to fight against drug-resistant cancers.[26] Therefore, we retained the main pharmacophore of sorafenib and tried to introduce hydrazone moiety and an indole ring at the tail part to provide additional interactions between the molecule and the amino acid residues. To further analyze the structure-activity relationship (SAR) on the tail part, the electronic effect of the aryl ring was investigated by introducing halogen or heterocycles with various electronics. Based on this design concept, a series of new derivatives were synthesized. Additionally, the cytotoxicity of tested compounds was evaluated by methyl thiazolyl tetrazolium (MTT) assay. The wound plate clone formation experiment, flow cytometry, reactive oxygen species (ROS) detection, propidium iodide (PI) staining experiment and western blot were applied to investigate the potential reasons regarding the compounds anticancer effect.

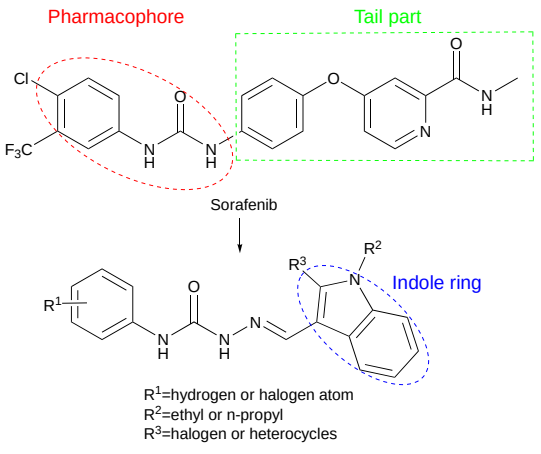

Figure 1. Design strategy of the target compounds

RESULTS AND DISCUSSION

Chemistry

The designed compound of sorafenib derivatives with indole was depicted in **Scheme 1**. The key intermediate *N*-phenylhydrazinecarboxamide **C** can be achieved from corresponding aromatic amines via a two-step protocol including amidation and hydrazidation. Compound **D** was further treated with an excess of phosphorus oxychloride to produce 2-chloro-1*H*-indole-3-carbaldehyde **E** in moderate under conventional ice bath conditions. These on further reaction with haloalkanes and acetone yield the compounds **F**. Treatment of compound **C** with indole-3-carbaldehyde derivatives **F**, **G** gave compounds **1-30** in good yield. The structures of compounds **1-30** were confirmed by ^{1}H NMR, ^{13}C NMR and HRMS spectral studies (Supporting Information).

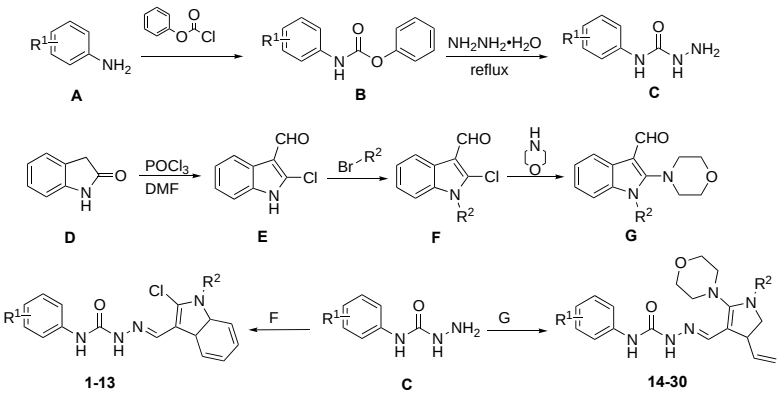

1 R^1=H, R^2=C_3H_7;
2 R^1=3-F, R^2=C_3H_7;
3 R^1=4-F, R^2=C_3H_7;
4 R^1=3,4-di-F, R^2=C_3H_7;
5 R^1=3,5-di-F, R^2=C_3H_7;
6 R^1=3-Cl, R^2=C_3H_7;
7 R^1=2,4-di-Cl, R^2=C_3H_7;
8 R^1=4-OMe, R^2=C_3H_7;
9 R^1=4-Me, R^2=C_3H_7;
10 R^1=3-CF_3-4-Cl, R^2=C_3H_7;
11 R^1=3,4-di-F, R^2=C_2H_5;
12 R^1=3,5-di-F, R^2=C_2H_5;
13 R^1=4-Me, R^2=C_2H_5;
14 R^1=4-F, R^2=C_2H_5;
15 R^1=3,4-di-F, R^2=C_2H_5;
16 R^1=3,5-di-F, R^2=C_2H_5;
17 R^1=3-Cl, R^2=C_2H_5;
18 R^1=2-F, R^2=C_2H_5;
19 R^1=4-Me, R^2=C_2H_5;
20 R^1=3-CF_3-4-Cl, R^2=C_2H_5;
21 R^1=H, R^2=C_2H_5;
22 R^1=4-OMe, R^2=C_3H_7;
23 R^1=3-CF_3-4-Cl, R^2=C_3H_7;
24 R^1=3,4-di-F, R^2=C_3H_7;
25 R^1=4-Me, R^2=C_3H_7;
26 R^1=2-F, R^2=C_3H_7;
27 R^1=3-Cl, R^2=C_3H_7;
28 R^1=3,5-di-F, R^2=C_3H_7;
29 R^1=4-F, R^2=C_3H_7;
30 R^1=H, R^2=C_3H_7.

Scheme 1. Synthetic route of the target compounds

Biological activity

Evaluation of cytotoxicity

The cytotoxicity of synthetic compounds *in vitro* against four human cancer cell lines was evaluated by MTT assay. The cytotoxicity results of 30 compounds in the indole series at a concentration of 10 μmol/L (μM) are shown in Table **S1**. Compounds **4**, **6**, **9**, **10**, **15**, **20**, **23**, **24**, and **26** against human lung cancer cell (A549), human prostate cancer cell (PC-3) and human liver cancer cell (HepG2) had relatively good inhibitory effects overall, while the effect on human chronic myeloid leukemia cell (K562) was relatively weak. Afterwards, we measured the IC_{50} of these compounds against the above three kinds of cancer cells and rat renal tubular epithelial cells (NRK-52E) by using MTT method. The results are shown in Table **1**. It is not difficult to find that the activity of compound **4** is not only better than **2** and **3**, but also better than

5, indicating that the *ortho* substitution on the benzene ring is better than the *meta* substitution. The trifluoromethyl substituent in compound **10** also made the compound have a good antitumor activity. The fact that the activity of compound **12** is also better than that of **5** indicates that the ethyl substitution at the 1-position of indole may be better than the propyl substitution. In contrast, compound **11** and compound **4** both had good activity, which may mean that benzene with 3,4-difluoro substituent on the ring is not greatly affected by the length of the alkyl carbon chain at the 1-position of the indole compounds. Compared with the first 13 molecules, the design of compounds **14-30** introduced a morpholine group at the indole 2-position. Among them, compounds **15**, **16**, **18**, **20**, **23**, **24**, and **29** had outstanding activity on HepG2, which indicated that the morpholine group introduced at the 2-position may dedicate the compound's inhibitory on HepG2. These compounds were both benzene ring with 4-fluoro substituted, compound **29** had better antitumor activity than **3**. And the overall activities of compounds **28** and **16** are better than compound **5**, indicating that compared with chlorine substitution, the introduction of morpholine groups may increase the benzene ring on 4-fluoro and 3,5-difluoro substituted activity.

The antitumor activity results encouraged us to study the mechanism of antitumor activity using ELISA-based EGFR-TK assay with sorafenib as the reference drug. The IC_{50} values of the tested compounds were calculated and are listed in **Table 1**. Compared to sorafenib reference drug (IC_{50}=0.71±0.02 μM), compound **4** and **6** revealed worthy EGFR inhibition activity with IC_{50} value of 0.47±0.04 and 0.13±0.01 μM, respectively. These data indicated that **6** was worth to further investigation.

In addition, compound **6** and compound **4** have similar tumor suppressor activity, but the toxicity to normal cells is lower than that of compound **4**. In order to further verify the inhibitory effect of compound **6** on cancer cells, a plate clone formation experiment was performed on the population dependence and proliferation ability of PC-3 cells by crystal violet staining. The results are shown in **Figure S91**. After compound **6** stimulation, cell cloning ability is obviously inhibited. Therefore, compound **6** was selected for further in-depth study of the mechanism.

Table 1. IC_{50} Values for EGFRwt-TK, human cancer cells and normal cell

Comp.	IC_{50}[a]±SD/(μmol/L)				
	A549	PC-3	HepG2	NRK-52E	$EGFR^{wt}$-TK
4	9.18±0.25	6.75±1.48	16.68±4.60	15.23±4.89	0.47±0.04
6	12.38±0.41	8.03±0.96	17.66±2.15	21.33±6.22	0.13±0.01
9	13.71±1.11	11.48±5.11	16.67±2.33	24.20±1.43	3.05±0.06
10	14.84±0.80	11.83±1.56	6.97±1.40	26.0±11.60	2.04±0.06
15	13.04±0.99	11.96±0.82	10.55±1.58	27.74±4.84	ND[b]
20	13.67±1.9	8.77±0.87	11.95±2.06	36.00±0.84	4.84±0.30

23	13.27±1.92	14.74±0.88	8.65±0.76	9.71±1.26	2.30±0.05
24	11.67±1.60	12.91±1.76	15.44±7.91	32.37±8.63	ND
26	9.54±0.33	15.89±1.03	22.40±2.68	19.73±3.08	9.53±0.23
Sorafenib[c]	24.15±1.91	18.92±2.02	11.66±1.75	46.14±6.00	0.71±0.02

[a]Average of the three trials. [b] Not determined. [c] Commercial sorafenib was used as positive control.

Apoptosis and mitochondrial dysfunction of compound 6

In order to investigate whether the inhibitory effect of compound **6** on PC-3 cell proliferation is related to apoptosis, we used Hoechst 33258 staining to evaluate the changes in PC-3 cell morphology after compound **6** treatment (**Figure 2A**). Compound **6** caused obvious damage to the karyotype of PC-3 cells, but the appearance of apoptotic bodies was not obvious. The decrease of cell mitochondrial membrane potential is a sign of apoptosis. Therefore, in order to determine that compound **6** can induce cell apoptosis, we used JC−1 fluorescent probe to detect the effect of compound **6** on cell mitochondrial function. Normal mitochondria will show strong red fluorescence, while abnormal cell mitochondria will produce green fluorescence due to the drop or loss of membrane potential. As expect, compound **6** induced a decrease in the mitochondrial membrane potential of PC-3 cells in a dose-dependent manner, as evidenced by the increase of green/red fluorescence intensity (**Figure 2B**).

Next, we did a quantitative analysis of the apoptosis caused by compound **6** by flow cytometry. The test results of different concentrations of compound in PC-3 cells for 24 and 48 h are shown in **Figure 2C**. When the concentration of compound **6** is 0 μM, 5 μM, 10 μM, and 20 μM, the apoptosis rates are as follows: 6.5%, 8.14%, 11.1%, 18.21%, and when the drug is applied for 48 h, the number of apoptosis increased significantly by about 2−3 times. Obviously, compound **6** promoted PC-3 cell apoptosis in a time and concentration dependent manner.

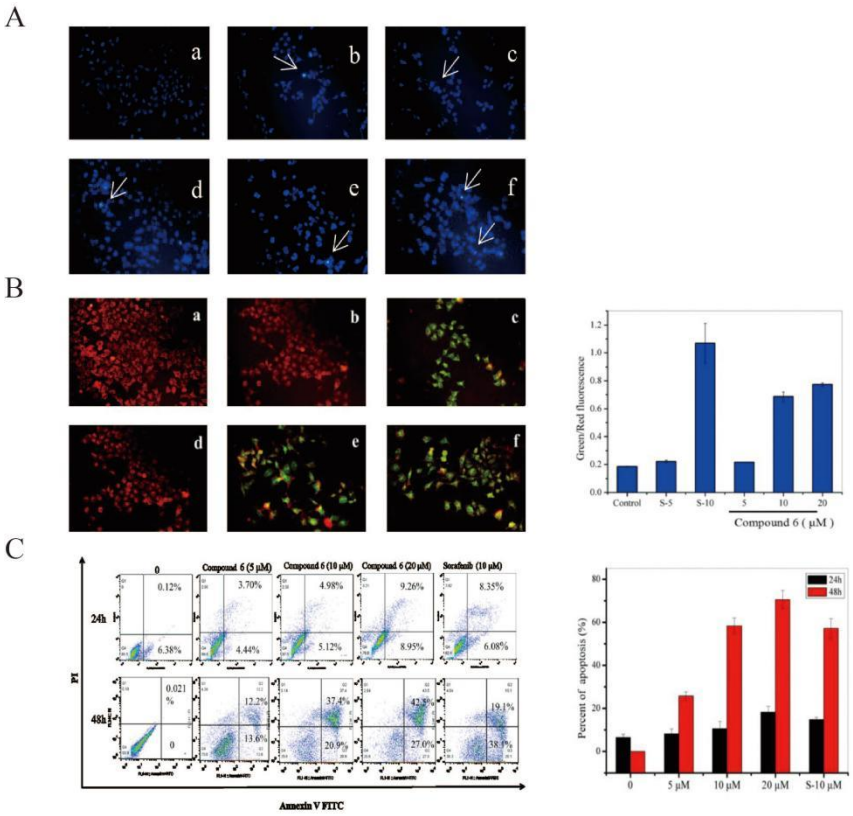

Figure 2. Apoptosis and mitochondrial dysfunction of compound **6**

A. Hoechst 33258 staining results of compound **6** and sorafenib. a. Control negative group. b. 5 μM sorafenib treatment for 24 h. c. 10 μM sorafenib treatment for 24 h. d. 5 μM compound **6** treatment for 24 h. e. 10 μM compound **6** treatment for 24 h. f. 20 μM compound **6** treatment for 24 h. B. JC−1 staining experiment: a. Control negative group. b. 5 μM sorafenib treatment for 24 h. c. 10 μM sorafenib treatment for 24 h. d. 5 μM compound **6** treatment for 24 h. e. 10 μM compound **6** treatment for 24 h. f. 20 μM compound **6** treatment for 24 h. C. Apoptosis graphs and statistical graphs of compound **6** and sorafenib.

Reactive oxygen species of compound 6

The different level of intracellular ROS can be used as a potential strategy for the development of anticancer drugs with high therapeutic indicators.[27,28] When ROS increases to a certain level, it may suppress the antioxidant capacity of cells and trigger cell death. Compared with normal cells, the level of reactive oxygen species for compounds **6** in most cancer cells is relatively higher.[29]

We used the fluorescent probe DCFH-DA to detect the changes in ROS levels in PC-3 cells after treatment with compound **6** (**Figure 3**). Compared with negative control, the ROS levels in cells treated with sorafenib and different concentrations of compound **6** were significantly increased. At low concentration (5 μM), the effect of compound **6** is stronger than that of sorafenib, while at 10 μM, the effect of compound group is equivalent to that of sorafenib. In short, compound **6** can increase the level of ROS in the PC-3 cell.

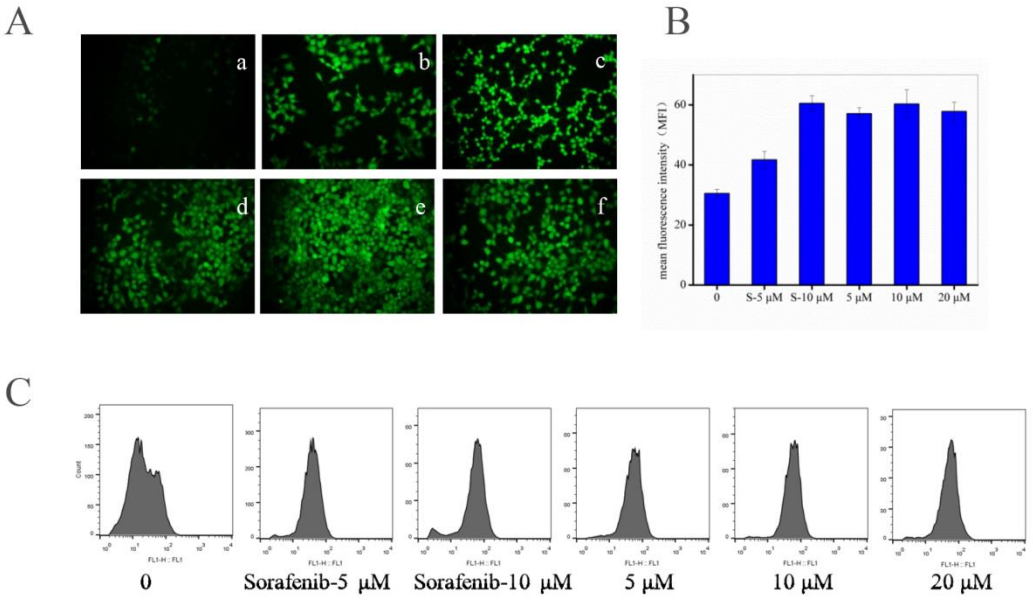

Figure 3. Level of reactive oxygen species of compound **6**

A. Fluorescence of ROS detection in PC-3 cells, the scale was 10 times. a. Control negative group b. Treat cells with 5 μM sorafenib for 24 h c. Treat cells with 10 μM sorafenib for 24 h d. 5 μM compound **6** treatment for 24 h e. 10 μM compound **6** treatment for 24 h f. 20 μM compound **6** treatment for 24 h B. Flow cytometry graph of ROS levels in PC-3 cells C. Statistical graph of the mean fluorescence intensity (MFI) of ROS levels in PC-3 cells.

Analysis of cell cycle of compound 6

Taking sorafenib as a control, different concentrations (0, 5, 10, and 20 μM) of compound **6** were applied to PC-3 cells for 24 and 48 h. The test results are shown in **Figure 4**. When applied for 24 h later, as the compound concentration increased, the G1 phase showed a decreasing trend (66.0%, 58.1%, and 58.2%, respectively), while the G2/M phase showed an upward trend (15.2%, 17.6%, and 18.0%, respectively). When the compound was treated for 48 h, the cell G1 phase decreased from 55.0% to 47.3%, 46.5%, 38.4%, and the percentage of G2/M phase increased from 11.2% to 16.2%, 17.0%, 21.0%. The mode of action is the same as that of 24 h, and it is also blocked in the G2/M phase, but the intensity of the action is enhanced. These results indicated that compound **6** can induce the PC-3 cells cycle arrest at the G2/M phase.

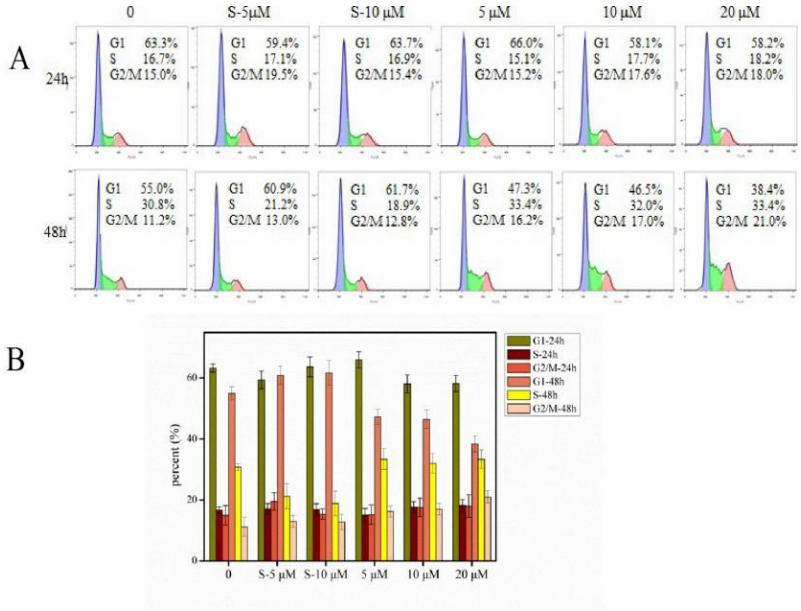

Figure 4. The results of the cycle experiment

A. Cycle charts of PC-3 cells treated with compound **6** (0, 5, 10, 20 μM) and sorafenib (5, 10 μM) for 24, 48 h B. PC-3 cell cycle percentage chart.

Western blot

In order to further determine the mechanism of the compound's inhibitory effect on cancer cells, we used western blot to detect the compound's effect on the expression of related proteins, including the effects on EGFR, Akt and its phosphorylated proteins, at concentrations of 10 and 20 μM. The results are shown in **Figure 5**, similar to the effect of sorafenib that compound **6** can reduce the expression of Akt, p-Akt and p-EGFR. Low concentration of compound **6** can reduce the expression of EGFR, but high concentration had the opposite trend.

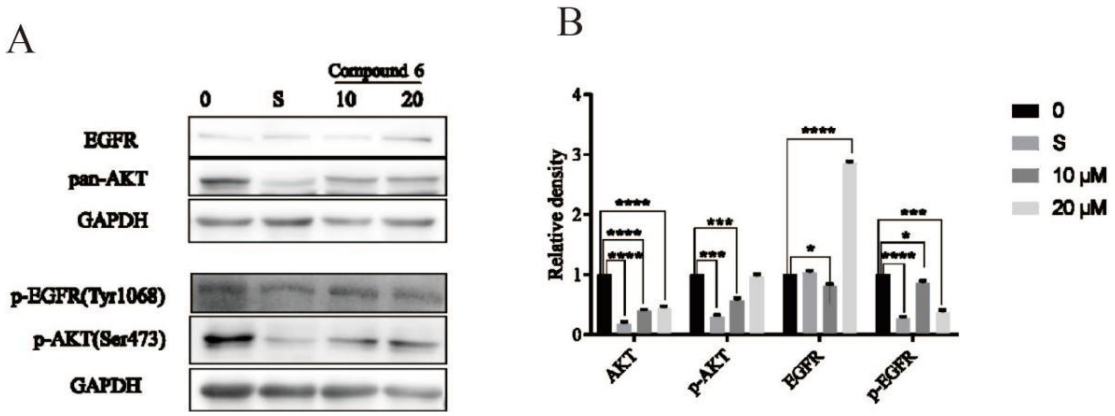

Figure 5. *In vitro* cellular phosphorylation assay of compound **6**

A. The influence of EGFR, Akt, p-EGFR and p-Akt proteins in PC-3 cells treated with indole series compound **6** (0, 10, 20 μM) and sorafenib (10 μM) B. Relative density statistics. * $p<0.05$, ** $p<0.01$, *** $p<0.001$, **** $p<0.0001$.

CONCLUSIONS

A new series of sorafenib derivatives containing indole (ketone) semicarbazide analogues were designed and synthesized. We tested the cytotoxicity of 30 compounds at a concentration of 10 μM by MTT method. A structure-activity relationship (SAR) study has been made to correlate between the structures and cytotoxicity activities. Results of the plate clone formation experiment proved that compound **6** had a strong inhibitory effect on the proliferation and colony formation ability of PC-3 cells. After that, we further evaluated the effect of the compound on the apoptosis of the corresponding cancer cells. The results showed that compound **6** induces PC-3 cell apoptosis in a concentration-dependent manner, and the comparison of compound **6** inducing PC-3 apoptosis for 24 and 48 h shows that the action time is longer. The apoptotic rate is significantly increased by more than 50%. Since the level of reactive oxygen species in most cancer cells is higher than that in normal cells, we used the fluorescent probe DCFH-DA to evaluate the effect of compounds on the level of ROS in cancer cells. The results showed that compound **6** increased the levels of ROS in PC-3 cells. In the next cell cycle experiment, the results showed that compound **6** blocked PC-3 cells in G2/M phase.

We combined a large amount of previous literature and research to simulate the interaction between compound **6** and the possible protein target EGFRwt through western blot. The results showed that compound **6** can reduce Akt, p-Akt and p-EGFR. Therefore, we speculate that compound **6** affects the signal transduction of the downstream signaling pathway PI3K/Akt by affecting the activity of the EGFR protein itself and its autophosphorylation, thereby regulating cell proliferation, differentiation, migration, and apoptosis and other life activities.

In conclusion, among the 30 new indole derivatives synthesized, compound **6** showed effective anticancer activity against PC-3 cells. The results of *in vitro* experiments also show the potential of compound **6** as a potential antitumor small molecule inhibitor, and the exact mechanism of action is worthy of in-depth study.

EXPERIMENTAL

Materials

All reagents were purchased from commercial sources as analytical grade and were used without further purification. ^{1}H NMR and ^{13}C NMR spectra were performed on a Bruker Ascend 400 NMR spectrometer and JEOL-ECX 500 NMR spectrometer using deuterated dimethyl sulfoxide (DMSO-d_6) as solvent and TMS as internal standard. High-resolution mass spectra (HRMS) were recorded on Thermo Scientific Q Extractive series with an ESI source. Melting points (°C) were obtained on an X-4D Micro melting point apparatus. Inverted fluorescence microscope (Nikon, Japan), carbon dioxide incubator (thermo, USA), enzyme labeling instrument (Tecan, Switzerland). Cell lines: A549 (Kunming cell bank of Chinese

Academy of Sciences), PC-3 (Kunming cell bank of Chinese Academy of Sciences), HepG2 (Kunming cell bank of Chinese Academy of Sciences), K562 (Kunming cell bank of Chinese Academy of Sciences).

Chemistry

Synthesis of variant carbamate (B)

To the mixture of variant amines (50.0 mmol) and K_2CO_3 (13.8 g, 0.100 mol) in acetone (50 mL), phenyl chloroformate (75.0 mmol) was added dropwisely while maintaining the temperature between 0 and 5 °C. After the addition was completed, the mixture was warmed to room temperature for another 3 h, and the solvent was evaporated under reduced pressure. The residue was washed with water 50 mL for thrice, filtered, and dried under vacuum to afford corresponding carbamates B.

Synthesis of *N*-phenylhydrazinecarboxamide (C)

A mixture of an appropriate carbamate B (20.0 mmol) and 80% hydrazine hydrate (10 mL) in 1,4-dioxane (10 mL) was refluxed overnight with vigorous agitation. After cooling to room temperature, the resulting precipitate was filtered-off, washed with water, and dried under vacuum to afford corresponding semicarbazides C.

General procedure for synthesis of 2-chloro-1*H*-indole-3-carbaldehyde (E)

Indolin-2-one (45 mmol) was added to a solution of $POCl_3$ (107 mmol) dropwise in DMF (30 mL) at 0 °C, then the reaction mixture was stirred to room temperature. After stirring for 24 h, the mixture was poured into ice water (350 mL). The mixture was filtered and the obtained solids were recrystallized from EtOH to give 2-chloro-1*H*-indole-3-carbaldehyde (E).

General procedure for synthesis of 2-chloro-1-ethyl-1*H*-indole-3-carbaldehyde (F)

Put 2-chloro-1*H*-indole-3-carbaldehyde (E) (27.84 mmol) in acetone (140 mL), was added dropwise bromoethane (36.19 mmol) and added sodium carbonate (41.76 mmol), then the reaction mixture was stirred at room temperature. After stirring for 2 h, the reaction mixture was evaporated under the reduced pressure, and subsequently diluted with water. The mixture was filtered and the obtained solids were recrystallized from EtOH to give 2-chloro-1-ethyl-1*H*-indole-3-carbaldehyde (F).

General procedure for synthesis of 1-ethyl-2-morpholino-1*H*-indole-3-carbaldehyde (G)

A mixture of 1-(4-*tert*-butylphenyl)-2-chloro-1*H*-indole-3-carboxaldehyde (3 g, 14.45 mmol), piperazine (16.36 g, 187.81 mmol) in dioxane (60 mL) is heated overnight at 110 °C. Then, added water, filtered and recrystallized from MeOH.

General procedure for synthesis of (*E*)-2-((1-ethyl-2-morpholino-1*H*-indol-3-yl)methylene)-*N*-phenylhydrazine-1-carboxamide (1-30)

1*H*- Indole-3-carboxaldehyde (0.99 mmol) was taken into a round bottom flask and to it added an equimolar quantity (0.99 mmol) of *p*-substituted arylsemicarbazides. The reaction mixture was refluxed in EtOH for

about 3 h. The resultant compound was allowed to stand for 30 min. Then cooled in ice. The product was filtered and recrystallized from EtOH.

((2-Chloro-1-propyl-1*H*-indol-3-yl)methylene)-*N*-phenylhydrazine-1-carboxamide (1)

Yellow solid, mp 147−148 °C, yield 62%; ^{1}H NMR (500 MHz, DMSO-d_6) δ 10.54 (s, 1H), 8.54 (s, 1H), 8.26 – 8.23 (m, 1H), 8.19 (s, 1H), 7.60 – 7.56 (m, 3H), 7.30 – 7.26 (m, 3H), 7.23 (td, *J* = 7.7, 1.1 Hz, 1H), 7.01 – 6.97 (m, 1H), 4.22 (t, *J* = 7.1 Hz, 2H), 1.72 (dd, *J* = 14.5, 7.3 Hz, 2H), 0.83 (t, *J* = 7.4 Hz, 3H). ^{13}C NMR (101 MHz, DMSO-d_6) δ 153.38 (s), 139.56 (s), 136.63 (s), 135.95 (s), 129.08 (s), 128.17 (s), 123.60 (s), 122.87 (s), 122.06 (s), 121.90 (s), 119.99 (s), 110.81 (s), 107.59 (s), 45.19 (s), 23.01 (s), 11.39 (s). HRMS (ESI) calcd for $C_{19}H_{19}ClN_4O$ $[M+H]^+$ 355.13202, found 355.13141.

2-((2-Chloro-1-propyl-1*H*-indol-3-yl)methylene)-*N*-(3-fluorophenyl)hydrazine-1-carboxamide (2)

White solid, mp 153−154 °C, yield 58%; ^{1}H NMR (500 MHz, DMSO-d_6) δ 10.63 (s, 1H), 8.78 (s, 1H), 8.28 – 8.25 (m, 1H), 8.19 (s, 1H), 7.60 (ddd, *J* = 15.2, 7.5, 5.2 Hz, 2H), 7.38 (dd, *J* = 8.2, 1.0 Hz, 1H), 7.31 – 7.18 (m, 3H), 6.84 – 6.74 (m, 1H), 4.22 (t, *J* = 7.1 Hz, 2H), 1.76 – 1.67 (m, 2H), 0.83 (t, *J* = 7.4 Hz, 3H). ^{13}C NMR (101 MHz, DMSO-d_6) δ 163.93 (s), 161.54 (s), 153.26 (s), 141.56 (d, *J* = 11.2 Hz), 137.13 (s), 135.94 (s), 130.53 (d, *J* = 9.7 Hz), 128.34 (s), 123.60 (d, *J* = 4.3 Hz), 122.06 (s), 115.73 (d, *J* = 2.2 Hz), 110.76 (s), 109.08 (d, *J* = 21.1 Hz), 107.53 (s), 106.67 (s), 106.41 (s), 45.20 (s), 23.00 (s), 11.38 (s). HRMS (ESI) calcd for $C_{19}H_{18}ClFN_4O$ $[M+H]^+$ 373.12259, found 373.12201.

2-((2-Chloro-1-propyl-1*H*-indol-3-yl)methylene)-*N*-(4-fluorophenyl)hydrazine-1-carboxamide (3)

White solid, mp 189−190 °C, yield 61%; ^{1}H NMR (500 MHz, DMSO-d_6) δ 10.54 (s, 1H), 8.61 (s, 1H), 8.28 (d, *J* = 7.8 Hz, 1H), 8.18 (s, 1H), 7.62 – 7.56 (m, 3H), 7.29 – 7.24 (m, 1H), 7.23 – 7.19 (m, 1H), 7.14 – 7.09 (m, 2H), 4.22 (t, *J* = 7.1 Hz, 2H), 1.76 – 1.67 (m, 2H), 0.83 (t, *J* = 7.4 Hz, 3H). ^{13}C NMR (101 MHz, DMSO-d_6) δ 162.76 (s), 159.43 (s), 157.06 (s), 153.57 (s), 136.75 (s), 135.96 (s), 135.93 (s), 128.20 (s), 123.59 (d, *J* = 1.5 Hz), 122.12 (s), 122.05 (s), 122.01 (s), 115.60 (s), 115.38 (s), 110.74 (s), 107.59 (s), 45.19 (s), 23.00 (s), 11.38 (s). HRMS (ESI) calcd for $C_{19}H_{18}ClFN_4O$ $[M-H]^+$ 371.10694, found 371.10794.

2-((2-Chloro-1-propyl-1*H*-indol-3-yl)methylene)-*N*-(3,4-difluorophenyl)hydrazine-1-carboxamide (4)

Yellow solid, mp 177−178 °C, yield 76%; ^{1}H NMR (500 MHz, DMSO-d_6) δ 10.61 (s, 1H), 8.79 (s, 1H), 8.29 (d, *J* = 7.9 Hz, 1H), 8.19 (s, 1H), 7.79 (ddd, *J* = 13.5, 7.5, 2.5 Hz, 1H), 7.57 (d, *J* = 8.2 Hz, 1H), 7.36 (ddd, *J* = 19.5, 13.6, 7.8 Hz, 2H), 7.29 – 7.25 (m, 1H), 7.24 – 7.20 (m, 1H), 4.22 (t, *J* = 7.2 Hz, 2H), 1.76 – 1.68 (m, 2H), 0.84 (t, *J* = 7.4 Hz, 3H). ^{13}C NMR (101 MHz, DMSO-d_6) δ 153.40 (s), 137.23 (s), 136.98 – 136.86 (m), 136.86 – 136.73 (m), 135.93 (s), 128.39 (s), 123.63 (s), 123.55 (s), 122.23 (s), 122.04 (s), 117.60 (s), 117.43 (s), 116.45 (s), 110.74 (s), 109.17 (s), 108.95 (s), 107.51 (s), 45.21 (s), 23.00 (s), 11.39 (s). HRMS (ESI) calcd for $C_{19}H_{17}ClF_2N_4O$ $[M+H]^+$ 391.11317, found 391.11261.

2-((2-Chloro-1-propyl-1*H*-indol-3-yl)methylene)-*N*-(3,5-difluorophenyl)hydrazine-1-carboxamide (5)

Yellow solid, mp 197−198 °C, yield 48%; ^{1}H NMR (500 MHz, DMSO-d_6) δ 10.70 (s, 1H), 8.98 (s, 1H), 8.30 – 8.27 (m, 1H), 8.21 (s, 1H), 7.57 (d, *J* = 8.0 Hz, 1H), 7.43 (dt, *J* = 6.6, 3.2 Hz, 2H), 7.30 – 7.26 (m, 1H), 7.25 – 7.20 (m, 1H), 6.80 (tt, *J* = 9.3, 2.3 Hz, 1H), 4.22 (t, *J* = 7.1 Hz, 2H), 1.76 – 1.68 (m, 2H), 0.83 (t, *J* = 7.4 Hz, 3H). ^{13}C NMR (101 MHz, DMSO-d_6) δ 164.18 (s), 164.02 (s), 161.77 (s), 161.62 (s), 153.14 (s), 137.64 (s), 135.92 (s), 128.54 (s), 123.66 (s), 123.54 (s), 122.25 (s), 122.09 (s), 110.74 (s), 107.45 (s), 102.79 (s), 102.49 (s), 45.21 (s), 22.98 (s), 11.38 (s). HRMS (ESI) calcd for $C_{19}H_{17}ClF_2N_4O$ $[M+H]^+$ 391.11317, found 391.11246.

2-((2-Chloro-1-propyl-1*H*-indol-3-yl)methylene)-*N*-(3-chlorophenyl)hydrazine-1-carboxamide (6)

White solid, mp 203−204 °C, yield 65%; ^{1}H NMR (500 MHz, DMSO-d_6) δ 10.64 (s, 1H), 8.77 (s, 1H), 8.30 – 8.27 (m, 1H), 8.20 (s, 1H), 7.84 (t, *J* = 2.0 Hz, 1H), 7.56 (d, *J* = 8.2 Hz, 1H), 7.54 – 7.49 (m, 1H), 7.32 – 7.20 (m, 3H), 7.03 (ddd, *J* = 8.0, 2.0, 0.8 Hz, 1H), 4.21 (t, *J* = 7.1 Hz, 2H), 1.71 (dd, *J* = 14.4, 7.3 Hz, 2H), 0.83 (t, *J* = 7.4 Hz, 3H). ^{13}C NMR (101 MHz, DMSO-d_6) δ 153.29 (s), 141.27 (s), 137.18 (s), 135.92 (s), 133.40 (s), 130.60 (s), 128.37 (s), 123.63 (s), 123.55 (s), 122.41 (s), 122.16 (s), 122.05 (s), 119.35 (s), 118.56 (s), 110.76 (s), 107.52 (s), 45.20 (s), 23.00 (s), 11.39 (s). HRMS (ESI) calcd for $C_{19}H_{18}Cl_2N_4O$ $[M-2]^+$ 387.07739, found 387.07864.

2-((2-Chloro-1-propyl-1*H*-indol-3-yl)methylene)-*N*-(2,4-dichlorophenyl)hydrazine-1-carboxamide (7)

Brown solid, mp 168−168 °C, yield 56%; ^{1}H NMR (500 MHz, DMSO-d_6) δ 11.00 (s, 1H), 8.78 (s, 1H), 8.36 (d, *J* = 8.9 Hz, 1H), 8.21 (s, 1H), 8.20 (d, *J* = 7.9 Hz, 1H), 7.67 (d, *J* = 2.4 Hz, 1H), 7.60 (d, *J* = 8.3 Hz, 1H), 7.41 (dd, *J* = 8.9, 2.4 Hz, 1H), 7.30 – 7.26 (m, 1H), 7.17 (dd, *J* = 11.2, 4.0 Hz, 1H), 4.22 (t, *J* = 7.1 Hz, 2H), 1.75 – 1.67 (m, 2H), 0.83 (t, *J* = 7.4 Hz, 3H). ^{13}C NMR (101 MHz, DMSO-d_6) δ 153.42 (s), 153.26 (s), 137.13 (s), 136.98 (s), 136.48 (s), 135.94 (s), 131.73 (s), 129.47 (s), 128.34 (s), 128.11 (s), 123.59 (s), 122.05 (s), 121.87 (s), 120.08 (s), 110.79 (s), 107.57 (d, *J* = 6.6 Hz), 45.19 (s), 23.00 (s), 20.86 (s). HRMS (ESI) calcd for $C_{19}H_{17}Cl_3N_4O$ $[M+H]^+$ 423.05407, found 423.05334.

2-((2-Chloro-1-propyl-1*H*-indol-3-yl)methylene)-*N*-(4-methoxyphenyl)hydrazine-1-carboxamide (8)

White solid, mp 191−192 °C, yield 59%; ^{1}H NMR (500 MHz, DMSO-d_6) δ 10.45 (s, 1H), 8.39 (s, 1H), 8.26 (d, *J* = 7.7 Hz, 1H), 8.17 (s, 1H), 7.56 (d, *J* = 8.2 Hz, 1H), 7.49 – 7.45 (m, 2H), 7.29 – 7.24 (m, 1H), 7.23 – 7.19 (m, 1H), 6.88 – 6.84 (m, 2H), 4.21 (t, *J* = 7.1 Hz, 2H), 3.70 (s, 3H), 1.71 (dd, *J* = 14.4, 7.3 Hz, 2H), 0.83 (t, *J* = 7.4 Hz, 3H). ^{13}C NMR (101 MHz, DMSO-d_6) δ 155.43 (s), 153.65 (s), 136.36 (s), 135.93 (s), 132.56 (s), 128.05 (s), 123.58 (s), 122.11 (s), 122.01 (s), 114.24 (s), 110.75 (s), 107.64 (s), 55.67 (s), 45.18 (s), 23.01 (s), 11.39 (s). HRMS (ESI) calcd for $C_{20}H_{21}ClN_4O_2$ $[M+H]^+$ 385.14313, found 385.14200.

2-((2-Chloro-1-propyl-1*H*-indol-3-yl)methylene)-*N*-(*p*-tolyl)hydrazine-1-carboxamide (9)

Brown solid, mp 191−192 °C, yield 68%; ^{1}H NMR (500 MHz, DMSO-d_6) δ 10.50 (s, 1H), 8.43 (s, 1H), 8.25 – 8.23 (m, 1H), 8.18 (s, 1H), 7.57 (d, *J* = 8.0 Hz, 1H), 7.48 – 7.45 (m, 2H), 7.29 – 7.25 (m, 1H), 7.23

(td, *J* = 7.7, 1.1 Hz, 1H), 7.08 (d, *J* = 8.2 Hz, 2H), 4.21 (t, *J* = 7.1 Hz, 2H), 2.23 (s, 3H), 1.75 – 1.67 (m, 2H), 0.83 (t, *J* = 7.4 Hz, 3H). ^{13}C NMR (101 MHz, DMSO-*d*$_6$) δ 153.42 (s), 153.26 (s), 137.13 (s), 136.98 (s), 136.48 (s), 135.94 (s), 131.73 (s), 129.47 (s), 128.34 (s), 128.11 (s), 123.59 (s), 122.05 (s), 121.87 (s), 120.08 (s), 110.79 (s), 107.57 (d, *J* = 6.6 Hz), 45.19 (s), 23.00 (s), 20.86 (s). HRMS (ESI) calcd for $C_{20}H_{21}ClN_4O$ $[M-H]^+$ 367.13202, found 367.13324.

2-((2-Chloro-1-propyl-1*H*-indol-3-yl)methylene)-*N*-(4-chloro-3-(trifluoromethyl)phenyl)hydrazine-1-carboxamide (10)

Brown solid, mp 193−194 °C, yield 50%; ^{1}H NMR (500 MHz, DMSO-*d*$_6$) δ 10.72 (s, 1H), 9.09 (d, *J* = 7.1 Hz, 1H), 8.33 (t, *J* = 7.8 Hz, 1H), 8.28 (d, *J* = 5.2 Hz, 1H), 8.22 (d, *J* = 7.9 Hz, 1H), 7.90 (d, *J* = 6.7 Hz, 1H), 7.59 (dt, *J* = 15.6, 8.2 Hz, 2H), 7.30 – 7.19 (m, 2H), 4.25 – 4.20 (m, 2H), 1.72 (dt, *J* = 14.5, 7.3 Hz, 2H), 0.84 (dd, *J* = 14.8, 7.3 Hz, 3H). ^{13}C NMR (101 MHz, DMSO-*d*$_6$) δ 154.07 – 150.37 (m), 137.03 – 136.51 (m), 136.01 (s), 132.56 – 131.79 (m), 128.79 – 128.42 (m), 127.51 – 127.33 (m), 125.26 – 124.77 (m), 123.73 (s), 123.50 (s), 122.05 (s), 121.30 (s), 121.16 – 120.74 (m), 115.85 – 115.51 (m), 115.55 – 115.28 (m), 112.65 – 109.85 (m), 108.05 – 106.12 (m), 45.23 (s), 23.01 (s), 11.41 (s). HRMS (ESI) calcd for $C_{20}H_{17}Cl_2F_3N_4O$ $[M+H]^+$ 457.08043, found 457.07974.

***N*-(4-Fluorophenyl)-2-((2-morpholino-1-propyl-1*H*-indol-3-yl)methylene)hydrazine-1-carboxamide (11)**

White solid, mp 185−186 °C, yield 76%; ^{1}H NMR (400 MHz, DMSO-*d*$_6$) δ 10.36 (s, 1H), 8.52 (d, *J* = 7.5 Hz, 2H), 8.22 – 8.18 (m, 1H), 7.66 – 7.61 (m, 2H), 7.45 (d, *J* = 7.7 Hz, 1H), 7.23 – 7.12 (m, 4H), 4.11 (t, *J* = 7.2 Hz, 2H), 3.78 (s, 4H), 3.19 (d, *J* = 10.2 Hz, 4H), 1.71 (dd, *J* = 14.5, 7.3 Hz, 2H), 0.87 (t, *J* = 7.4 Hz, 3H). ^{13}C NMR (101 MHz, DMSO-*d*$_6$) δ 159.32 (s), 156.95 (s), 153.53 (s), 148.82 (s), 138.43 (s), 136.04 (s), 134.06 (s), 124.22 (s), 122.75 (s), 122.23 (s), 121.75 (s), 121.67 (s), 121.22 (s), 115.65 (s), 115.43 (s), 110.72 (s), 103.51 (s), 67.54 (s), 52.40 (s), 43.85 (s), 23.25 (s), 11.78 (s). HRMS (ESI) calcd for $C_{23}H_{26}FN_5O_2$ [M+H]+ 424.21433, found 424.21375.

2-((1-Ethyl-2-morpholino-1*H*-indol-3-yl)methylene)-*N*-(4-fluorophenyl)hydrazine-1-carboxamide (12)

Brown solid, mp 189−190 °C, yield 57%; ^{1}H NMR (500 MHz, DMSO-*d*$_6$) δ 10.31 (s, 1H), 8.48 (d, *J* = 2.9 Hz, 2H), 8.17 (d, *J* = 7.9 Hz, 1H), 7.62 – 7.58 (m, 2H), 7.41 (d, *J* = 7.9 Hz, 1H), 7.20 – 7.16 (m, 1H), 7.15 – 7.09 (m, 3H), 4.16 (d, *J* = 7.2 Hz, 2H), 3.75 (s, 4H), 3.18 (s, 4H), 1.24 (t, *J* = 7.1 Hz, 3H). ^{13}C NMR (101 MHz, DMSO-*d*$_6$) δ 153.53 (s), 148.46 (s), 138.47 (s), 136.02 (d, *J* = 2.3 Hz), 133.68 (s), 124.36 (s), 122.77 (s), 122.26 (s), 121.74 (s), 121.66 (s), 121.25 (s), 115.54 (d, *J* = 22.1 Hz), 115.27 – 113.01 (m), 110.45 (s), 103.53 (s), 67.56 (s), 52.34 (s), 36.75 (d, *J* = 101.6 Hz), 15.57 (s). HRMS (ESI) calcd for $C_{22}H_{24}FN_5O_2$ $[M+H]^+$ 410.19923, found 410.19800.

***N*-(3,4-Difluorophenyl)-2-((1-ethyl-2-morpholino-1*H*-indol-3-yl)methylene)hydrazine-1-carboxamide (13)**

Yellow solid, mp 158−159 °C, yield 67%; ^{1}H NMR (500 MHz, DMSO-d_6) δ 10.46 (s, 1H), 8.93 (s, 1H), 8.51 (s, 1H), 8.28 (d, *J* = 2.6 Hz, 1H), 8.25 – 8.19 (m, 1H), 7.88 (dd, *J* = 8.8, 2.5 Hz, 1H), 7.60 (d, *J* = 8.8 Hz, 1H), 7.40 (d, *J* = 8.1 Hz, 1H), 7.16 (dtd, *J* = 14.9, 7.6, 1.1 Hz, 2H), 4.16 (q, *J* = 7.1 Hz, 2H), 3.76 (s, 4H), 3.19 (s, 4H), 1.25 (t, *J* = 7.1 Hz, 3H). ^{13}C NMR (101 MHz, DMSO-d_6) δ 153.35 (s), 148.63 (s), 138.95 (s), 133.69 (s), 124.33 (s), 122.80 (s), 122.42 (s), 121.27 (s), 117.65 (s), 117.48 (s), 116.13 (s), 110.43 (s), 108.86 (s), 108.64 (s), 103.46 (s), 67.57 (s), 52.37 (s), 37.27 (s), 15.56 (s). HRMS (ESI) calcd for $C_{22}H_{23}F_2N_5O_2$ $[M+H]^+$ 428.18981, found 428.18863.

2-((2-Chloro-1-ethyl-1*H*-indol-3-yl)methylene)-*N*-(3,5-difluorophenyl)hydrazine-1-carboxamide (14)

White solid, mp 122−123 °C, yield 49%; ^{1}H NMR (400 MHz, DMSO-d_6) δ 10.74 (s, 1H), 9.02 (s, 1H), 8.33 (d, *J* = 7.3 Hz, 1H), 8.25 (s, 1H), 7.60 (d, *J* = 8.0 Hz, 1H), 7.51 – 7.43 (m, 2H), 7.35 – 7.24 (m, 2H), 6.84 (tt, *J* = 9.3, 2.1 Hz, 1H), 4.33 (q, *J* = 7.0 Hz, 2H), 1.29 (t, *J* = 7.1 Hz, 3H). ^{13}C NMR (101 MHz, DMSO-d_6) δ 164.08 (d, *J* = 15.6 Hz), 161.68 (d, *J* = 15.6 Hz), 153.15 (s), 142.56 (t, *J* = 14.3 Hz), 137.55 (s), 135.35 (s), 128.10 (s), 123.66 (d, *J* = 5.1 Hz), 122.36 (s), 122.11 (s), 110.48 (s), 107.52 (s), 102.79 (s), 102.50 (s), 97.59 (t, *J* = 26.2 Hz), 15.14 (s). HRMS (ESI) calcd for $C_{18}H_{15}ClF_2N_4O$ $[M+H]^+$ 377.09752, found 377.09702.

2-((2-Chloro-1-ethyl-1*H*-indol-3-yl)methylene)-*N*-(*p*-tolyl)hydrazine-1-carboxamide (15)

White solid, mp 175−176 °C, yield 78%; ^{1}H NMR (400 MHz, DMSO-d_6) δ 10.54 (s, 1H), 8.47 (s, 1H), 8.31 – 8.25 (m, 1H), 8.21 (s, 1H), 7.60 (d, *J* = 7.8 Hz, 1H), 7.50 (d, *J* = 8.4 Hz, 2H), 7.29 (dtd, *J* = 19.0, 7.3, 1.2 Hz, 2H), 7.12 (d, *J* = 8.3 Hz, 2H), 4.32 (q, *J* = 7.1 Hz, 2H), 2.27 (s, 3H), 1.29 (t, *J* = 7.1 Hz, 3H). ^{13}C NMR (101 MHz, DMSO-d_6) δ 153.42 (s), 136.97 (s), 136.41 (s), 135.36 (s), 131.72 (s), 129.47 (s), 127.68 (s), 123.66 (d, *J* = 4.2 Hz), 122.08 (s), 121.98 (s), 120.12 (s), 110.56 (s), 107.66 (s), 38.81 (s), 20.87 (s), 15.16 (s). HRMS (ESI) calcd for $C_{19}H_{19}ClN_4O$ $[M+H]^+$ 355.13202, found 355.13135.

***N*-(3,5-Difluorophenyl)-2-((1-ethyl-2-morpholino-1*H*-indol-3-yl)methylene)hydrazine-1-carboxamide (16)**

White solid, mp 176−177 °C, yield 65%; ^{1}H NMR (400 MHz, DMSO-d_6) δ 10.51 (s, 1H), 8.88 (s, 1H), 8.53 (s, 1H), 8.25 – 8.19 (m, 1H), 7.46 (dd, *J* = 13.0, 5.1 Hz, 3H), 7.20 (ddt, *J* = 8.3, 7.2, 3.5 Hz, 2H), 6.82 (tt, *J* = 9.3, 2.3 Hz, 1H), 4.19 (q, *J* = 7.1 Hz, 2H), 3.79 (s, 4H), 3.22 (s, 4H), 1.28 (t, *J* = 7.1 Hz, 3H). ^{13}C NMR (101 MHz, DMSO-d_6) δ 164.06 (s), 161.65 (s), 153.08 (s), 148.72 (s), 142.62 (t, *J* = 14.3 Hz), 139.31 (s), 133.68 (s), 124.32 (s), 122.82 (s), 122.45 (s), 121.32 (s), 110.41 (s), 103.40 (s), 102.55 (s), 102.26 (s), 97.46 (t, *J* = 26.2 Hz), 67.56 (s), 52.35 (s), 37.28 (s), 15.55 (s). HRMS (ESI) calcd for $C_{22}H_{23}F_2N_5O_2$ $[M+H]^+$ 428.18981, found 428.18863.

***N*-(3-Chlorophenyl)-2-((1-ethyl-2-morpholino-1*H*-indol-3-yl)methylene)hydrazine-1-carboxamide (17)**

White solid, mp 145−146 °C, yield 62%; ^{1}H NMR (400 MHz, DMSO-d_6) δ 10.45 (s, 1H), 8.67 (s, 1H), 8.52 (s, 1H), 8.23 – 8.18 (m, 1H), 7.88 (t, *J* = 2.0 Hz, 1H), 7.53 (dd, *J* = 8.2, 1.2 Hz, 1H), 7.44 (d, *J* = 7.5 Hz, 1H), 7.33 (t, *J* = 8.1 Hz, 1H), 7.25 – 7.15 (m, 2H), 7.06 (ddd, *J* = 8.0, 2.0, 0.7 Hz, 1H), 4.19 (d, *J* = 7.1 Hz, 2H), 3.79 (s, 4H), 3.22 (s, 4H), 1.28 (t, *J* = 7.1 Hz, 3H). ^{13}C NMR (101 MHz, DMSO-d_6) δ 153.24 (s), 148.59 (s), 141.32 (s), 138.90 (s), 133.69 (s), 133.46 (s), 130.65 (s), 124.35 (s), 122.80 (s), 122.29 (s), 121.29 (s), 119.06 (s), 118.25 (s), 110.45 (s), 103.46 (s), 67.56 (s), 52.35 (s), 36.76 (d, *J* = 103.6 Hz), 15.57 (s). HRMS (ESI) calcd for $C_{22}H_{24}ClN_5O_2$ $[M+H]^+$ 426.16913, found 426.16846.

2-((1-Ethyl-2-morpholino-1*H*-indol-3-yl)methylene)-*N*-(2-fluorophenyl)hydrazine-1-carboxamide (18)

White solid, mp 158−159 °C, yield 59%; ^{1}H NMR (500 MHz, DMSO-d_6) δ 10.22 (s, 1H), 8.46 (s, 1H), 8.27 (s, 1H), 8.14 (d, *J* = 7.9 Hz, 1H), 7.48 – 7.45 (m, 2H), 7.41 (d, *J* = 8.0 Hz, 1H), 7.20 – 7.11 (m, 2H), 6.88 – 6.84 (m, 2H), 4.16 (q, *J* = 7.1 Hz, 2H), 3.75 (s, 4H), 3.18 (s, 4H), 1.24 (t, *J* = 7.1 Hz, 3H). ^{13}C NMR (101 MHz, DMSO-d_6) δ 155.28 (s), 153.62 (s), 148.33 (s), 138.08 (s), 133.66 (s), 132.64 (s), 124.36 (s), 122.76 (s), 122.14 (s), 121.69 (s), 121.24 (s), 114.26 (s), 110.49 (s), 103.56 (s), 67.57 (s), 55.65 (s), 52.33 (s), 15.60 (s). HRMS (ESI) calcd for $C_{22}H_{24}FN_5O_2$ $[M+Na]^+$ 432.18062, found 432.18292.

2-((1-Ethyl-2-morpholino-1*H*-indol-3-yl)methylene)-*N*-(*p*-tolyl)hydrazine-1-carboxamide (19)

White solid, mp 178−179 °C, yield 54%; ^{1}H NMR (400 MHz, DMSO-d_6) δ 10.30 (s, 1H), 8.50 (s, 1H), 8.36 (s, 1H), 8.18 – 8.14 (m, 1H), 7.50 (d, *J* = 8.4 Hz, 2H), 7.44 (d, *J* = 7.4 Hz, 1H), 7.25 – 7.16 (m, 2H), 7.12 (d, *J* = 8.3 Hz, 2H), 4.19 (q, *J* = 7.0 Hz, 2H), 3.79 (s, 4H), 3.22 (s, 4H), 2.27 (s, 3H), 1.28 (t, *J* = 7.1 Hz, 3H). ^{13}C NMR (101 MHz, DMSO-d_6) δ 153.40 (s), 148.37 (s), 138.19 (s), 137.05 (s), 133.68 (s), 131.57 (s), 129.52 (s), 124.39 (s), 122.77 (s), 122.00 (s), 121.28 (s), 119.72 (s), 110.52 (s), 103.52 (s), 67.56 (s), 52.32 (s), 36.75 (d, *J* = 100.6 Hz), 20.85 (s), 15.58 (s). HRMS (ESI) calcd for $C_{23}H_{27}N_5O_2$ $[M+H]^+$ 406.22430, found 406.22324.

***N*-(4-Chloro-3-(trifluoromethyl)phenyl)-2-((1-ethyl-2-morpholino-1*H*-indol-3-yl)methylene)hydrazine-1-carboxamide (20)**

White solid, mp 155−156 °C, yield 46%; ^{1}H NMR (500 MHz, DMSO-d_6) δ 10.38 (s, 1H), 8.65 (s, 1H), 8.49 (s, 1H), 8.20 – 8.14 (m, 1H), 7.80 (ddd, *J* = 13.5, 7.4, 2.4 Hz, 1H), 7.43 – 7.27 (m, 3H), 7.21 – 7.09 (m, 2H), 4.16 (q, *J* = 7.1 Hz, 2H), 3.75 (s, 4H), 3.18 (s, 4H), 1.25 (t, *J* = 7.1 Hz, 3H). ^{13}C NMR (101 MHz, DMSO-d_6) δ 153.32 (s), 148.74 (s), 139.52 (s), 139.33 (s), 133.70 (s), 132.15 (s), 124.79 (d, *J* = 11.4 Hz), 124.32 (s), 122.82 (s), 122.55 (s), 121.24 (s), 110.40 (s), 103.45 (s), 67.57 (s), 52.39 (s), 37.28 (s), 15.55 (s). HRMS (ESI) calcd for $C_{23}H_{23}ClF_3N_5O_2$ $[M-H]^+$ 492.14086, found 492.14188.

2-((1-Ethyl-2-morpholino-1*H*-indol-3-yl)methylene)-*N*-phenylhydrazine-1-carboxamide (21)

White solid, mp 210−211 °C, yield 43%; ^{1}H NMR (400 MHz, DMSO-d_6) δ 10.35 (s, 1H), 8.52 (s, 1H), 8.46 (s, 1H), 8.17 (dd, *J* = 7.0, 1.6 Hz, 1H), 7.64 – 7.60 (m, 2H), 7.47 – 7.42 (m, 1H), 7.32 (dd, *J* = 10.8, 5.1 Hz, 2H), 7.25 – 7.16 (m, 2H), 7.02 (t, *J* = 7.4 Hz, 1H), 4.19 (d, *J* = 7.2 Hz, 2H), 3.79 (s, 4H), 3.22 (s, 4H), 1.28 (t, *J* = 7.1 Hz, 3H). ^{13}C NMR (101 MHz, DMSO-d_6) δ 153.34 (s), 148.43 (s), 139.61 (s), 138.35 (s), 133.69 (s), 129.14 (s), 124.40 (s), 122.76 (d, *J* = 4.1 Hz), 122.02 (s), 121.30 (s), 119.64 (s), 110.54 (s), 103.49 (s), 67.56 (s), 52.33 (s), 37.26 (s), 15.58 (s). HRMS (ESI) calcd for $C_{22}H_{25}N_5O_2$ $[M+H]^+$ 392,20865, found 392.20755.

***N*-(4-Methoxyphenyl)-2-((2-morpholino-1-propyl-1*H*-indol-3-yl)methylene)hydrazine-1-carboxamide (22)**

Yellow solid, mp 162−163 °C, yield 53%; ^{1}H NMR (400 MHz, DMSO-d_6) δ 10.26 (s, 1H), 8.50 (s, 1H), 8.31 (s, 1H), 8.17 (d, *J* = 7.4 Hz, 1H), 7.50 (d, *J* = 9.0 Hz, 2H), 7.45 (d, *J* = 7.9 Hz, 1H), 7.18 (ddd, *J* = 14.9, 13.9, 6.5 Hz, 2H), 6.89 (d, *J* = 9.0 Hz, 2H), 4.11 (s, 2H), 3.78 (s, 4H), 3.73 (s, 3H), 3.26 – 3.14 (m, 4H), 1.71 (dd, *J* = 14.5, 7.3 Hz, 2H), 0.87 (t, *J* = 7.4 Hz, 3H). ^{13}C NMR (101 MHz, DMSO-d_6) δ 155.28 (s), 153.62 (s), 148.68 (s), 138.04 (s), 134.06 (s), 132.66 (s), 124.26 (s), 122.72 (s), 122.08 (s), 121.67 (s), 121.20 (s), 114.27 (s), 110.75 (s), 103.55 (s), 67.54 (s), 55.66 (s), 52.37 (s), 43.85 (s), 23.25 (s), 11.78 (s). HRMS (ESI) calcd for $C_{24}H_{29}N_5O_3$ $[M+H]^+$ 436.23432, found 436.23398.

***N*-(4-Chloro-3-(trifluoromethyl)phenyl)-2-((2-morpholino-1-propyl-1*H*-indol-3-yl)methylene)hydrazine-1-carboxamide (23)**

Yellow solid, mp 156−157 °C, yield 62%; ^{1}H NMR (400 MHz, DMSO-d_6) δ 10.51 (s, 1H), 8.98 (s, 1H), 8.54 (s, 1H), 8.32 (d, *J* = 2.5 Hz, 1H), 8.26 (d, *J* = 7.4 Hz, 1H), 7.91 (dd, *J* = 8.8, 2.5 Hz, 1H), 7.64 (d, *J* = 8.8 Hz, 1H), 7.44 (d, *J* = 7.9 Hz, 1H), 7.19 (dtd, *J* = 14.8, 7.6, 1.1 Hz, 2H), 4.11 (t, *J* = 7.2 Hz, 2H), 3.78 (s, 4H), 3.21 (s, 4H), 1.77 – 1.67 (m, 2H), 0.87 (t, *J* = 7.4 Hz, 3H). ^{13}C NMR (101 MHz, DMSO-d_6) δ 153.32 (s), 149.11 (s), 139.53 (s), 139.29 (s), 134.07 (s), 132.15 (s), 124.80 (d, *J* = 12.5 Hz), 124.18 (s), 122.78 (s), 122.53 (s), 121.21 (s), 110.67 (s), 103.43 (s), 67.54 (s), 52.45 (s), 43.88 (s), 23.22 (s), 11.76 (s). HRMS (ESI) calcd for $C_{24}H_{25}ClF_3N_5O_2$ $[M+H]^+$ 508.17216, found 508.17197.

***N*-(3,4-Difluorophenyl)-2-((2-morpholino-1-propyl-1*H*-indol-3-yl)methylene)hydrazine-1-carboxamide (24)**

Brown solid, mp 121−122 °C, yield 43%; ^{1}H NMR (400 MHz, DMSO-d_6) δ 10.43 (s, 1H), 8.70 (s, 1H), 8.53 (s, 1H), 8.24 – 8.20 (m, 1H), 7.84 (ddd, *J* = 13.6, 7.4, 2.2 Hz, 1H), 7.47 – 7.32 (m, 3H), 7.23 – 7.14 (m, 2H), 4.10 (t, *J* = 7.2 Hz, 2H), 3.78 (s, 4H), 3.20 (s, 4H), 1.71 (dd, *J* = 14.5, 7.3 Hz, 2H), 0.87 (t, *J* = 7.4 Hz, 3H). ^{13}C NMR (101 MHz, DMSO-d_6) δ 153.35 (s), 150.81 – 147.07 (m), 138.89 (s), 134.07 (s), 124.22 (s), 122.76 (s), 122.36 (s), 121.24 (s), 117.64 (s), 117.47 (s), 116.07 (s), 110.67 (s), 108.84 (s), 108.62 (s),

103.46 (s), 67.53 (s), 52.40 (s), 43.87 (s), 23.23 (s), 11.75 (s). HRMS (ESI) calcd for $C_{23}H_{25}F_2N_5O_2$ $[M+H]^+$ 442.20546, found 442.20432.

2-((2-Morpholino-1-propyl-1*H*-indol-3-yl)methylene)-*N*-(*p*-tolyl)hydrazine-1-carboxamide (25)

White solid, mp 156−157 °C, yield 50%; ^{1}H NMR (400 MHz, DMSO-d_6) δ 10.31 (s, 1H), 8.50 (s, 1H), 8.36 (s, 1H), 8.15 (dd, *J* = 7.0, 1.6 Hz, 1H), 7.49 (d, *J* = 8.4 Hz, 2H), 7.47 – 7.41 (m, 1H), 7.23 – 7.15 (m, 2H), 7.12 (d, *J* = 8.3 Hz, 2H), 4.11 (t, *J* = 7.1 Hz, 2H), 3.78 (s, 4H), 3.28 – 3.10 (m, 4H), 2.27 (s, 3H), 1.71 (dd, *J* = 14.5, 7.3 Hz, 2H), 0.87 (t, *J* = 7.4 Hz, 3H). ^{13}C NMR (101 MHz, DMSO-d_6) δ 153.40 (s), 148.74 (s), 138.16 (s), 137.05 (s), 134.07 (s), 131.57 (s), 129.52 (s), 124.27 (s), 122.74 (s), 121.96 (s), 121.25 (s), 119.72 (s), 110.79 (s), 103.50 (s), 67.54 (s), 52.37 (s), 43.86 (s), 23.25 (s), 20.86 (s), 11.78 (s). HRMS (ESI) calcd for $C_{24}H_{29}N_5O_2$ $[M+H]^+$ 420.23940, found 420.23898.

***N*-(2-Fluorophenyl)-2-((2-morpholino-1-propyl-1*H*-indol-3-yl)methylene)hydrazine-1-carboxamide (26)**

Yellow solid, mp 197−198 °C, yield 67%; ^{1}H NMR (400 MHz, DMSO-d_6) δ 10.61 (s, 1H), 8.55 (s, 2H), 8.22 (td, *J* = 8.2, 1.6 Hz, 1H), 8.10 (d, *J* = 7.8 Hz, 1H), 7.48 (d, *J* = 8.1 Hz, 1H), 7.32 (ddd, *J* = 11.4, 8.2, 1.3 Hz, 1H), 7.19 (dtd, *J* = 15.8, 7.6, 1.0 Hz, 3H), 7.10 – 7.03 (m, 1H), 4.11 (t, *J* = 7.2 Hz, 2H), 3.78 (s, 4H), 3.21 (s, 4H), 1.72 (dd, *J* = 14.5, 7.3 Hz, 2H), 0.88 (t, *J* = 7.4 Hz, 3H). ^{13}C NMR (101 MHz, DMSO-d_6) δ 152.73 (s), 150.10 – 148.72 (m), 138.83 (s), 134.30 (s), 125.27 – 124.98 (m), 124.02 (s), 123.44 – 123.27 (m), 123.27 – 123.15 (m), 122.87 (s), 121.81 – 121.69 (m), 121.69 – 121.61 (m), 121.58 – 121.47 (m), 121.23 (s), 120.76 (s), 116.20 – 115.05 (m), 115.05 – 114.34 (m), 111.05 (s), 103.24 (s), 67.53 (s), 52.71 (s), 43.94 (s), 23.20 (s), 11.78 (s). HRMS (ESI) calcd for $C_{23}H_{26}FN_5O_2$ $[M+H]^+$ 424.21433, found 424.21396.

***N*-(3-Chlorophenyl)-2-((2-morpholino-1-propyl-1*H*-indol-3-yl)methylene)hydrazine-1-carboxamide (27)**

Brown solid, mp 156−157 °C, yield 60%; ^{1}H NMR (400 MHz, DMSO-d_6) δ 10.44 (s, 1H), 8.67 (s, 1H), 8.53 (s, 1H), 8.23 – 8.18 (m, 1H), 7.88 (t, *J* = 2.0 Hz, 1H), 7.53 (dd, *J* = 8.2, 1.2 Hz, 1H), 7.44 (d, *J* = 7.4 Hz, 1H), 7.33 (t, *J* = 8.1 Hz, 1H), 7.24 – 7.14 (m, 2H), 7.06 (ddd, *J* = 8.0, 2.0, 0.8 Hz, 1H), 4.11 (t, *J* = 7.2 Hz, 2H), 3.78 (s, 4H), 3.21 (s, 4H), 1.71 (dd, *J* = 14.5, 7.3 Hz, 2H), 0.87 (t, *J* = 7.4 Hz, 3H). ^{13}C NMR (101 MHz, DMSO-d_6) δ 153.24 (s), 148.94 (s), 141.32 (s), 138.85 (s), 134.07 (s), 133.46 (s), 130.65 (s), 124.24 (s), 122.77 (s), 122.28 (s), 121.26 (s), 119.05 (s), 118.24 (s), 110.71 (s), 103.46 (s), 67.53 (s), 52.39 (s), 43.88 (s), 23.24 (s), 11.77 (s). HRMS (ESI) calcd for $C_{23}H_{26}ClN_5O_2$ $[M+H]^+$ 440.18533, found 440.18436.

***N*-(3,5-Difluorophenyl)-2-((2-morpholino-1-propyl-1*H*-indol-3-yl)methylene)hydrazine-1-carboxamide (28)**

Yellow solid, mp 183−184 °C, yield 58%; ^{1}H NMR (400 MHz, DMSO-d_6) δ 10.51 (s, 1H), 8.88 (s, 1H), 8.53 (s, 1H), 8.21 (dd, *J* = 7.0, 1.6 Hz, 1H), 7.46 (dd, *J* = 12.9, 4.9 Hz, 3H), 7.24 – 7.12 (m, 2H), 6.82 (ddd,

J = 9.3, 5.8, 2.3 Hz, 1H), 4.11 (t, *J* = 7.1 Hz, 2H), 3.78 (s, 4H), 3.27 – 3.13 (m, 4H), 1.77 – 1.66 (m, 2H), 0.87 (t, *J* = 7.4 Hz, 3H). ^{13}C NMR (101 MHz, DMSO-*d*$_6$) δ 164.13 (d, *J* = 15.6 Hz), 161.73 (d, *J* = 15.6 Hz), 153.08 (s), 149.08 (s), 142.63 (t, *J* = 14.2 Hz), 139.26 (s), 134.06 (s), 124.21 (s), 122.78 (s), 122.41 (s), 121.29 (s), 110.68 (s), 103.38 (s), 102.55 (s), 102.25 (s), 97.46 (s), 67.53 (s), 52.40 (s), 43.88 (s), 23.22 (s), 11.76 (s). HRMS (ESI) calcd for $C_{23}H_{25}F_2N_5O_2$ $[M+H]^+$ 442.20491, found 442.20450.

2-((2-Chloro-1-ethyl-1*H*-indol-3-yl)methylene)-*N*-(3,4-difluorophenyl)hydrazine-1-carboxamide (29)

White solid, mp 162−163 °C, yield 71%; ^{1}H NMR (400 MHz, DMSO-*d*$_6$) δ 10.68 (s, 1H), 8.85 (s, 1H), 8.34 (d, *J* = 7.5 Hz, 1H), 8.23 (s, 1H), 7.83 (ddd, *J* = 13.5, 7.5, 2.4 Hz, 1H), 7.60 (d, *J* = 8.1 Hz, 1H), 7.46 – 7.23 (m, 4H), 4.32 (q, *J* = 7.1 Hz, 2H), 1.29 (t, *J* = 7.1 Hz, 3H). 13C NMR (101 MHz, DMSO-*d*$_6$) δ 153.41 (s), 137.02 (d, *J* = 27.3 Hz), 135.35 (s), 127.95 (s), 123.66 (d, *J* = 2.0 Hz), 122.33 (s), 122.06 (s), 117.60 (s), 117.43 (s), 116.47 (s), 110.48 (s), 109.17 (s), 108.96 (s), 107.57 (s), 38.83 (s), 15.15 (s). HRMS (ESI) calcd for $C_{18}H_{15}ClF_2N_4O$ $[M+H]^+$ 377.09752, found 377.09686.

2-((2-Morpholino-1-propyl-1*H*-indol-3-yl)methylene)-*N*-phenylhydrazine-1-carboxamide (30)

Yellow solid, mp 145−146 °C, yield 56%; ^{1}H NMR (400 MHz, DMSO-*d*$_6$) δ 10.31 (s, 1H), 8.50 (s, 1H), 8.36 (s, 1H), 8.15 (dd, *J* = 7.0, 1.6 Hz, 1H), 7.49 (d, *J* = 8.4 Hz, 2H), 7.47 – 7.41 (m, 1H), 7.23 – 7.15 (m, 2H), 7.12 (d, *J* = 8.3 Hz, 2H), 4.11 (t, *J* = 7.1 Hz, 2H), 3.78 (s, 4H), 3.28 – 3.10 (m, 4H), 2.27 (s, 3H), 1.71 (dd, *J* = 14.5, 7.3 Hz, 2H), 0.87 (t, *J* = 7.4 Hz, 3H). ^{13}C NMR (101 MHz, DMSO-*d*$_6$) δ 153.40 (s), 148.74 (s), 138.16 (s), 137.05 (s), 134.07 (s), 131.57 (s), 129.52 (s), 124.27 (s), 122.74 (s), 121.96 (s), 121.25 (s), 119.72 (s), 110.79 (s), 103.50 (s), 67.54 (s), 52.37 (s), 43.86 (s), 23.25 (s), 20.86 (s), 11.78 (s). HRMS (ESI) calcd for $C_{23}H_{27}N_5O_2$ $[M+H]^+$ 406.22375, found 406.22345.

Biological activity

MTT assay

Cells in logarithmic growth were cultured in a 96-well plate and preincubated for 24 h before accession the test compounds. Then 20 μL various concentrations of each compound solution were added in 96-well plate. After the cells were cultured for 48 h at 37 °C and 5% CO_2, MTT solution (20 μL of 5 μg/mL) was added to react in the same environment for 4 h. After the formazan crystals were dissolved in DMSO, the absorbance was measured at 490 nm with a microplate reader (Tecan, Infinite M200 Pro).

Clone formation assay

After the cells cultured in a 6-well plate were incubated with the compound solution of various concentrations for 24 h, they were each transferred to a new 6-well plate at a density of 1000 cells/well. The plate was continued to cultivate for about 2 weeks at 37 °C and 5% CO_2, during which the medium

was changed every 3 days. After the visible clumps were formed, the cells could be stained with 0.1% crystal violet solution in the dark for 30 min. After washing, the next was taking pictures and calculated the cloning rate (Cloning rate = Number of clones/Number of inoculations).

***In vitro* EGFR^{wt}-TK assay**

The effects of compounds on the activity of wild type EGFR tyrosine kinase were determined by enzyme-linked immunosorbent assays (ELISAs) with recombinant EGFR according to reported methods. Recombinant EGFR was purchased from Sino Biology Inc. Antiphosphotyrosine mouse mAb was purchased from PTM Bio. The EGFR kinase activities for each compound were expressed as IC_{50} values used five concentrations (1, 0.2, 0.04, 0.01 and 0.0016 μM).

Hoechst apoptosis experiment

After the adherent cells had stably grown in the 6-well plate, the test groups were reacted with compounds solution of different concentrations for 24 h, while the negative well was the same amount of DMSO. Then the cells could be fixed by 4% paraformaldehyde for 15 min, and added with 1 mL/well of dye for 20 min. After adding an anti-fluorescence quencher, cells could be imaged by an inverted fluorescence microscope.

JC−1 staining experiment

Cells in the logarithmic growth phase were planted in a 6-well plate. After 24 h, the required concentration of the drug was added and reacted in a 37 °C, 5% CO_2 incubator for 24 h. After washing with PBS twice, the prepared JC−1 staining working solution was added and incubated in the dark for 20 min. Then washing twice with JC−1 staining buffer, and imaging under red and green fluorescence.

ROS level detection experiment

Select cells that are in good condition and in the logarithmic growth phase were seeded in a 6-well plate, and allow them to adhere to and stably grow overnight. Then added the required concentration of compound solution to react for 24 h, and then remove the wells plate, discard the stock solution, add 1 mL of DCFH-DA solution diluted with basal medium (1:1000) per well, put it in an incubator and incubate in the dark for 20 min, discard the liquid, and wash carefully with basal medium 3 times to wash away the DCFH-DA that did not enter the cells, and finally develop the red and green fluorescence pictures under an inverted fluorescence microscope, and process the pictures with Image J software. When using a flow cytometer to detect the ROS level in cells, the steps are the same as the above seeding plate and the cells are treated with the corresponding concentration of compound for 24 h, then the cells are taken out, and the cells are collected one by one with a small 1.5 mL centrifuge tube, and centrifuged (1000 rpm/min, 5 min). Then discard the supernatant, add the diluted DCFH-DA solution (the same concentration as above), 1 mL per tube and fully resuspend. Place it in an incubator and incubate it in the dark for 20 min, paying attention to inverting and mixing every 3-4 min to make DCFH-DA fully contact the cells. After the incubation is

complete, centrifuge, discard the solution, add basal medium to resuspend, wash 3 times, and sieve the active oxygen levels in the cells can be detected on the flow cytometer. Use Flow Jo software to process the results, and repeat the experiment at least 3 times.

Flow cytometry apoptosis experiment

Apoptosis was assessed by flow cytometry of cells double-stained with Annexin V/FITC and PI. Treat PC-3 cells with or without the test compound at the specified concentration for 48 h. After 48 h, the cells were collected and washed twice with PBS, then the cells were resuspended in binding buffer, counted, and prepared 100 μL of cell suspension with a density of 106 cells/mL, and incubated with FITC Annexin V and PI (BD, Pharmingen) and stained in the dark for 15 min. Then add 400 μL of pre-cooled PBS, resuspend, and use Cell Quest software to perform detection on a flow cytometer (FAC Scan, Becton Dickenson). The system software (Cell Quest BD Biosciences) was used to analyze the apoptosis experiment.

Cell Cycle Analysis

PC-3 cells were grown in 6-well plates for 48 h at 37 °C in a humidified 5% CO_2, and then treated with or without the tested compounds at indicated concentrations. After co-incubated for 24 h, cells were collected and washed with ice-cold PBS two times, then fixed with 70% ethanol at 20 °C overnight. After centrifugation, 100 μL of RNase A was added to react for 30 min (water bath 37 °C), and then 400 μL of PI staining solution was added to incubate for 30 min in the dark. It can be tested on the flow cytometry (FAC Scan, Becton Dickenson) using Cell Quest software and recording PI in the FL2 channel.

Western Blot

The PC-3 cells in the logarithmic growth phase are selected to be seeded in a 6-well plate and incubated with or without the specified concentration of compound for 48 h. After incubation, the cells were washed twice with ice-cold PBS and then lysed in RIPA lysis buffer containing 150 mM NaCl, 50 mM Tris (pH 7.4), 1% (w/v) sodium deoxycholate, 1% (v/v) Triton X-100, 0.1% (w/v) SDS, and 1 mM EDTA (Beyotime, China). The lysates were incubated at 0 °C for 1 h and vortexed every 30 min intermittently, and then the total protein was harvested by centrifuging at 12,000 g for 15 min. After the protein concentrations were determined by a BCA Protein Assay Kit (Beyotime, China), the protein extracts were reconstituted in loading buffer containing 62 mM Tris-HCl, 2% SDS, 10% glycerol, and 5% β-mercaptoethanol (Beyotime, China) and boiled at 100 °C for 15 min. An equal amount of the proteins (40 μg) was separated by 8−12% sodium dodecyl sulfate-polyacrylamide gel electrophoresis (SDS-PAGE) and was transferred to nitrocellulose membranes. After blocked at room temperature for 90 min, add appropriate primary antibodies, included EGFR (CST11862, 1:800), phosphorylated p-EGFR (CST11862, 1:800), Akt (CST4691, 1:1000), p-Akt (CST4060, 1:2000) and GAPDH (proteintech HRP-60004, 1:20000) were sealed in Antibody Dilution Buffer (Beyotime, Shanghai, China), and cocultivated with the PVDF membrane at

4 °C overnight. After three washes in TBST, the membranes were incubated with the appropriate HRP-conjugated secondary antibodies at room temperature for 2 h. The blots were developed with enhanced chemiluminescence (Pierce, Rockford, Illinois, USA) and were detected by an imager.

REFERENCES

1. R. L. Siegel, K. D. Miller, and A. Jemal, *Ca-Cancer J. Clin.*, 2019, **69**, 7.
2. N. M. Raghavendra, D. Pingili, S. Kadasi, A. Mettu, and S. Prasad, *Eur. J. Med. Chem.*, 2018, **143**, 1277.
3. M. Mokhtar, K. S. Alghamdi, N. S. Ahmed, D. Bakhotmah, and T. S. Saleh, *J. Enzyme Inhib. Med. Chem.*, 2021, **36**, 1454.
4. P. Carmeliet and R. K. Jain, *Nature*, 2011, **473**, 298.
5. S. Wilhelm, C. Carter, M. Lynch, T. Lowinger, J. Dumas, R. A. Smith, B. Schwartz, R. Simantov, and S. Kelley, *Nat. Rev. Drug Discov.*, 2006, **5**, 835.
6. T. Guida, S. Anaganti, L. Provitera, R. Gedrich, E. Sullivan, S. M. Wilhelm, M. Santoro, and F. Carlomagno, *Clin. Cancer Res.*, 2007, **13**, 3363.
7. Z. Babic, M. Crkvencic, Z. Rajic, A. M. Mikecin, M. Kralj, J. Balzarini, M. Petrova, J. Vanderleyden, and B. Zorc, *Molecules*, 2012, **17**, 1124.
8. D. K. Guan, S. F. Sun, J. He, Z. P. Chen, X. K. Kong, N. N. Wang, J. W. Yao, and H. B. Wang, *Chin. J. Org. Chem.*, 2018, **38**, 1414.
9. H. J. Cho, M. I. El-Gamal, C. H. Oh, S. H. Lee, T. Sim, G. Kim, H. S. Choi, J. H. Choi, and K. H. Yoo, *Chem. Pharm. Bull.*, 2013, **61**, 747.
10. K. F. Chen, W. T. Tai, J. W. Huang, C. Y. Hsug, W. L. Cheng, A. L. Cheng, and C. W. Shiau, *Eur. J. Med. Chem.*, 2011, **46**, 2845.
11. J. W. Yao, J. Chen, Z. P. He, W. Sun, H. Fang, and W. F. Xu, *Med. Chem. Res.*, 2013, **22**, 3959.
12. S. M. Wilhelm, C. Carter, L. Tang, D. Wilkie, A. McNabola, H. Rong, C. Rong, X. M. Zhang, P. Vincent, M. McHugh, Y. C. Cao, J. Shujath, S. Gawlak, D. Eveleigh, B. Rowley, L. Liu, L. Adnane, M. Lynch, D. Auclair, I. Taylor, R. Gedrich, A. Voznesensky, B. Riedl, L. E. Post, G. Bollag, and P. A. Trail, *Cancer Res.*, 2004, **64**, 7099.
13. F. Ciardiello and G. Tortora, *Eur. J. Cancer*, 2003, **39**, 1348.
14. A. L. Harris, *Breast Cancer Res. Treat.*, 1994, **29**, 1.
15. A. Ayatia, S. Moghimia, S. Salarinejadb, M. Safavic, B. Pouramiria, and A. Foroumadi, *Bioorg. Chem.*, 2020, **93**, 103811.
16. F. Ciardiello, *Drugs*, 2000, **60**, 25.
17. S. Ozawa, L. G. Sheflin, and S. W. Spaulding, *Endocrinology*, 1991, **128**, 1396.

18. L. C. Ariel and G. Giuseppe, *Nat. Rev. Clin. Oncol.*, 2010, **7**, 360.
19. M. Q. Mahmood, S. D. Shukla, K. Dua, and M. D. Shastri, *Curr. Pharm. Des.*, 2017, **23**, 2314.
20. N. Matsuda, B. Lim, X. P. Wang, and N. T. M. Ueno, *Expert Opin. Invest. Drugs*, 2017, **26**, 463.
21. Y. X. Jiang, Y. Wang, M. H. Nie, D. J. Zhang, and X. Zhai, *Molecules*, 2016, **21**, 1572.
22. L. H. Shao, S. L. Fan, Y. F. Meng, Y. Y. Gan, W. B. Shao, Z. C. Wang, D. P. Chen, and G. P. Ouyang, *New J. Chem.*, 2021, **45**, 4626.
23. P. Çıkla-Süzgün and Ş. G. Küçükgüzel, *Mini-Rev. Med. Chem.*, 2019, **19**, 1427.
24. J. G. Cui, L. Liu, D. D. Zhao, C. F. Gan, X. Huang, Q, Xiao, B. B. Qi, L. Yang, and Y. M. Huang, *Steroids*, 2015, **95**, 32.
25. Y. C. Wan, Y. H. Li, C. X. Yan, and Z. L. Tang, *Eur. J. Med. Chem.*, 2019, **183**, 111691.
26. Y. S. Jia, X. Y. Wen, Y. F. Gong, and X. F. Wang, *Eur. J. Med. Chem.*, 2020, **200**, 112359.
27. K. Li, B. T. Wang, L. F. Zheng, K. Yang, Y. Y. Li, and D. He, *Bioorg. Med. Chem. Lett.*, 2018, **28**, 273.
28. N. Wang, Y. Wu, J. L. Bian, X. Qian, H. Z. Lin, H. P. Sun, Q. D. You, and X. Zhang, *J. Curr. Cancer Drug Targets*, 2017, **17**, 122.
29. Y. H. Yang, S. Karakhanova, W. Hartwig, J. G. D'Haese, P. P. Philippov, J. Werner, and A. V. Bazhin, *J. Cell. Physiol.*, 2016, **231**, 2570.